

The Effect of Variations of EEJ on the Ionospheric TEC at Different Longitudinal Sectors using Ground-based Observation

Cherkos, A. M.¹  | Nigussie, M.² 

1. **Corresponding Author**, Department of Physics, CNCS, Institute of Geophysics Space Science and Astronomy, Addis Ababa University, Addis Ababa, Ethiopia. E-mail: alexyc9@yahoo.com

2. Department of Physics, Washera Geospace and Radar Science Research Laboratory, Bahir Dar University, Bahir Dar, Ethiopia. E-mail: melessewnigussie@yahoo.com

(Received: 14 Nov 2022, Revised: 17 Dec 2022, Accepted: 20 Feb 2023, Published online: 5 March 2023)

Abstract

In this work, the longitudinal variations of equatorial electrojet (EEJ) and its effect on the diurnal behavior of the EIA during quiet days in the period of 2011- 2012 were investigated. EEJ has been estimated using a pair of ground-based magnetometers data from six longitudinal sectors, and the Global Positioning System (GPS) TEC have also been obtained at each longitudinal sector from three stations at Northern and Southern crests and trough regions. The statistical results show that the monthly mean variations of EIA crest are consistent with that of the strength of equatorial electrojet in most regions of the investigation. The mean EEJ and EIA crests are strongest around equinoctial months in the Peruvian and Southeast Asian sectors followed by the West African regions throughout the years investigated. The weakest EEJ peaks and TEC of EIA are observed over the Pacific sectors throughout the periods of investigation. The monthly mean characteristics of EEJ/counter electrojets (CEJ) and EIA are also presented. The results also show that the CEJ events occur more frequently in the Brazilian sectors followed by in the Peruvian and West African sectors. However, in most of the equinoctial months, the strongest equatorial EIA trough and weakest of EIA crests are observed in the Brazilian sector. The temporal extent of the well-developed EIA crest and its properties show a substantial dependence on the diurnal characteristics of the EEJ for each specific day.

Keywords: Equatorial electrojet, Equatorial Ionospheric anomaly, Longitudinal Variation.

1. Introduction

The spatio-temporal ionospheric irregularities are the main source of errors for users of modern satellite-based communication, navigation systems and geolocation applications with the equatorial region providing the worst-case builds (Paul et al., 2011). Understanding the fundamental processes governing the dynamics and plasma production, distribution and loss in the low/mid-latitudes region is also essential for space weather forecasting (Yizengaw & Moldwin, 2009). The low-latitude ionosphere is a highly dynamic environment that exhibits significant variations with local time, altitude, latitude, longitude, solar cycle, season and geomagnetic activity (Fejer, 1997; Fejer & Tracy, 2013). The ionosphere is continually influenced by several highly variable electrodynamic processes due to neutral winds through collisions with the ions. The motion of plasma keeping its fundamental properties, such as its collective

behavior and the state of quasi-neutrality generates the ionospheric electric field (Khadka et al., 2018). Interaction of winds with ionized particles inside the geomagnetic field can also create the electric field in the ionosphere. This dynamo-electric field drives the equatorial electrojet (EEJ) in the ionospheric *E* region and vertical plasma drift in the ionospheric *F* region (Fejer & Tracy, 2013; Zhang et al., 2020).

In the equatorial ionosphere, the eastward electric field with the mutually perpendicular geomagnetic field lines are responsible for the \mathbf{ExB} drift of plasma upwards to a higher altitudes around the geomagnetic equator and the subsequent diffusion down along the geomagnetic field lines due to the gravitational and pressure gradient forces (Tsai et al., 2001; Anderson et al., 2002, 2006; Dias et al., 2020). It results in the formation of a double-humped latitudinal distribution of ionization known as the

Cite this article: Cherkos, A. M., & Nigussie, M. (2023). The Effect of Variations of EEJ on the Ionospheric TEC at Different Longitudinal Sectors using Ground-based Observation. *Journal of the Earth and Space Physics*, 48(4), 197-220. DOI: <http://doi.org/10.22059/jesphys.2023.350185.1007464>

equatorial ionization anomaly (EIA). The two humps of ionization at about $15^{\circ} - 20^{\circ}$ on either sides of the magnetic equatorial latitude are known as the crests of the EIA. The depleted ionization region over the geomagnetic equator is called as the trough of the EIA. Quiet-time low latitude ionospheric plasma drifts are also driven mostly by dynamo action of thermospheric neutral winds of tidal origin and planetary waves from below (Abdu et al., 2006; Fejer and Tracy, 2013).

The EEJ is a band of non-uniform intense eastward ionospheric current located within a latitudinal extent of 3° on either sides of the dip equator at an altitude of 105-110 km above sea level (Chapman, 1951; Rabiou et al., 2017). Egedal was the first to notice it, and Chapman named it equatorial electrojet (EEJ) in 1951 (Basavaiah, 2012). It enhances the horizontal component of H-field during the daytime that is measured by magnetometers located within the magnetic equator region (Fambitakoye & Mayaud, 1976a, 1976b; Chandrasekhar et al., 2014). During magnetically quiet days, the flow of the EEJ system reverses direction, causing periods of westward current in the ionospheric E region (known as counter equatorial electrojet CEJ) and depressions in the H-field at equatorial stations (Gouin, 1962; Chandrasekhar et al., 2014; Soares et al., 2018). The CEJ is a dip-equator phenomenon in which the H component field drops below the mean midnight value at certain times of the day (Rastogi, 2004). The CEJ event was initially discovered while studying the magnetic records of the Ethiopian station Addis Ababa (Gouin, 1962). In our previous work (Alemayehu & Melesew, 2022), we have discussed the longitudinal variations of EEJ and its reversal CEJ in the eight different longitudinal sectors and have noticed that the CEJ in the East African and Brazilian regions are more pronounced.

As it is described, the zonal electric field is the driving force for the EEJ, CEJ, and EIA at the magnetic equator, and they may show a high degree of correlation between them (Stolle et al., 2008; Hajra et al., 2009). Thus, the EEJ and EIA are the most typical equatorial and low-latitude ionospheric phenomena, and the characteristics of EEJ

play a vital role in the electron density distribution over equatorial and low latitudes. During the past few decades, authors have also reported the possible relation between EEJ and ionospheric total electron content of EIA: for example (Iyer et al., 1976; Rastogi and Klobuchar 1990; Rama Rao et al., 2006; Bagiya et al., 2009) in the Indian equatorial anomaly regions, (Anderson et al., 2002, 2004) for the South American sector during the period of 1998–1999, (Chen et al., 2008), in the Pacific-Australian region during 1999 - 2003, and (Bolaji et al., 2017) over Africa and the Middle East during a year of deep minimum. Venkatesh et al. (2015) pointed out the role of EEJ in the day-to-day characteristics of the EIA in the Indian and Brazilian sectors. They also pointed out that the EEJ exhibits significant diurnal, seasonal, day-to-day and longitudinal variabilities. The authors also examined the characteristics of CEJ and its effect on the development of EIA in the Peruvian (Stolle et al., 2008; Zhang et al., 2020), East African sector (Mungufeni et al., 2018), and Indian region (Hajra et al., 2009; Pandey et al., 2018). To improve TEC estimates across the equatorial and low-latitude sectors, quantitative investigations on the effect of EEJ on EIA characteristic features over different locations during varied solar activity circumstances will be of great value (Venkatesh et al., 2015). They have also shown the dependence of EIA on the diurnal characteristics of EEJ, which gives us the opportunity to further validate the EEJ and EIA results in other regions simultaneously.

The studies described above indicate the importance of studying the monthly and seasonal characteristics of EEJ and its role on the variations of EIA in different regions and solar condition. Stolle et al. (2008) suggested that due to the large-scale longitudinal variation of both the EEJ and EIA, different relations are expected in other longitudinal sectors. Moreover, although many studies have been carried out, the variation of EEJ effects on northern and southern anomaly crests along the six longitudinal sectors during the quietest periods have not been simultaneously studied by using ground-based data. Therefore, in the present study, the characteristics of longitudinal variations of EEJ and its role on the variations of the

EIA crests at different regions are investigated using ground based magnetometers data (Table 1) and GPS ionospheric TEC available along the equatorial region of the six different longitudinal sectors of Peruvian, Brazilian, West-African, Indian, Southeast Asian and Pacific regions in the year between 2011 and 2012. Moreover, we are concerned with the behavior of the day-to-day variability in the EEJ/CEJ and its effect on the diurnal behavior of the EIA under quiet magnetic conditions only ($AP < 15$). This work may help to have a better explanation of the relation of EEJ-Sq relation and the mechanism that drives the MCEJ, and ACEJ relation, and their effect on the variations of on the TEC of EIA under quiet geomagnetic conditions which is still an open question despite several studies being done during the last decades.

2. Data Analysis

The TEC data used for this paper were obtained from three different chains of ground-based GPS-TEC receivers along the common longitudes with each of the EEJ stations of the Peruvian, Brazilian, African, Indian, Southeast Asian and Pacific regions to derive and analyzed the characteristic features of the EIA ($1 \text{ TECU} = 10^{16} \text{ electrons/m}^2$). The latitudinal range of the GPS receivers considered lies between $\sim 15^\circ\text{N}$ and $\sim 15^\circ\text{S}$, and in/around the magnetic

equator (between 6°N and 6°S) geomagnetic latitude along with the EEJ stations with the same longitudinal zone. The station names and codes as well as their geographic and geomagnetic coordinate of all the 23 GPS receivers are listed in Table 2. The GPS data used for this research were obtained from the receiver independent exchange (RINEX) data files of the receivers in the University Navstar Consortium (UNAVCO) network <https://www.unavco.org/data/gps-gnss/data-access-methods/data-access-methods.html> for 22 receiver stations, from CDDIS Archive explorer for KOUG station (https://cddis.nasa.gov/Data_and_Derived_Products/CddisArchiveExplorer.html), and from the Low Latitude ionospheric sensor Network (LISN) <http://lisn.igp.gob.pe/data/> for LHYO station (at Huancayo, Peru).

As depicted in Figure 1, the magnetic dip equator is indicated by a black bold line curve, while black thin lines above and below the dip-equator indicates 3° of latitude from the dip-equator. The cyan color thin lines above and below the dip-equator show probable EEJ zones (that is, between -6° and 6° magnetic latitude); the stations beyond the cyan color thin lines represent the off-the-dip equator. The solid red colored curve lines ($\sim \pm 15$ degree of latitude from the dip-equator) in Figure 1 indicate the region of the possible formation northern and southern equatorial ionization anomaly crest.

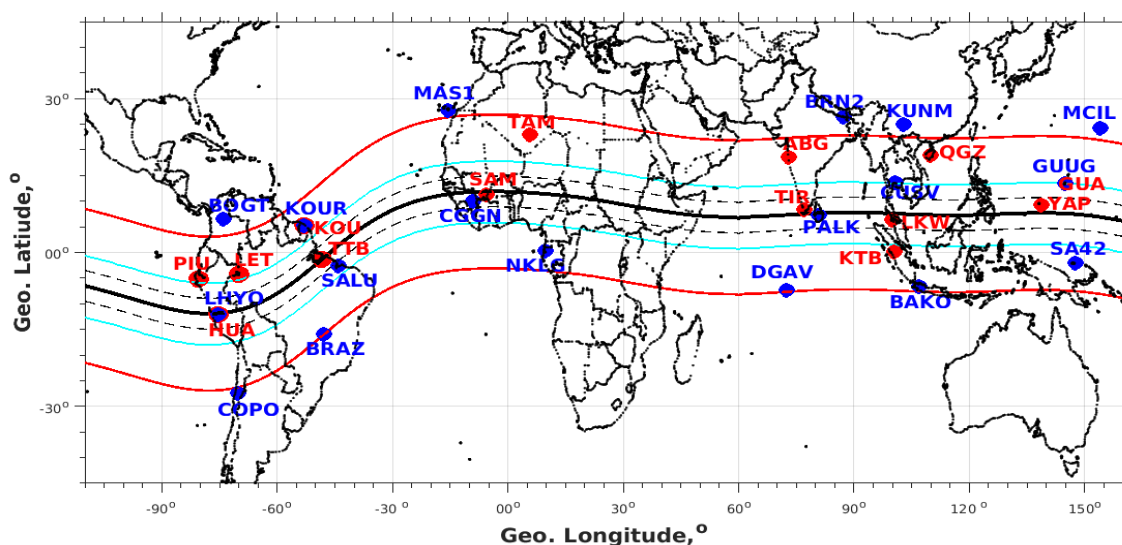


Figure 1. The Global map showing the geographical location of ground-based magnetometers (red circles) and the GPS receivers (blue circles) over Peruvian, Brazilian, African, Indian, South East Asian and Pacific sectors used in this study.

Table 1. List of Magnetometer stations used in this work.

Station Name	Station Code	Belongs to	Geog. Lat.	Geog. Long.	Geom. Lat .	Geom. Long.
Magnetometers Stations in the Peruvian Sector						
Huancayo	HUA	INTERMAGNET	12.1°S	75.3°W	0.14°S	357.33°E
Piura	PIU	IGP	5.2°S	80.6 °W	6.45 °N	352.23°E
Leticia	LET	LISN	4.2°S	69.9 °W	6.59 °N	3.33°W
Magnetometers Stations in the Brazilian Sector						
Tatuoca	TTB	WDC Catalogue	1.21°S	48.5 °W	0.19°N	24.27°E
Kourou	KOU	INTERMAGNET	5.21°N	53 °W	8.46°N	22.06°E
Magnetometers Stations in the West African Sector						
Samogossoni	SAM	WAMNET	11.39°N	5.62°W	0.54°S	68.82°E
Tamanrasset	TAM	INTERMAGNET	22.8°N	5.5°W	12.93°N	80.2°E
Magnetometers Stations in the Indian Sector						
Tirunelveli	TIR	SuperMAG	8.48°N	76.95°E	1.05°N	149.73°E
Alibag	ABG	INTERMAGNET	18.62°N	72.87°E	12.40°N	145.88°E
Magnetometers Stations in the Southeast Asian Sector						
Langkawi	LKW	SuperMAG	6.3°N	99.78°E	1.42°S	172.37°E
Kototabang	KTB	SuperMAG	0.2°S	100.3°E	8.55°S	172.81°E
BacLieu	BCL	SuperMAG	9.3°N	105.7°E	2.05°N	178.21°E
Qiongzhang	QGZ	WDC Catalogue	19°N	109.8°E	12.54°N	182.42°E
Magnetometers Stations in the Pacific Sector						
Yap	YAB	SuperMAG	9.3°N	138.5°E	1.66°N	210.65°E
Guam	GUA	INTERMAGNET	13.59°N	144.9°E	6.11°N	216.83°E

The list of calculated coordinates here are from the Geomagnetic coordinates IGRF-13 revised on Dec. 2019 (https://geomag.bgs.ac.uk/data_service/models_compass/coord_calc.html) at epoch = 2013.

2-1. Methodology

The station pair technique was utilized to isolate the EEJ effect during only geomagnetically quiet times using H-components data from ground-based magnetometers around the world. To achieve hourly values, the variance data acquired at 1 minute sampling intervals is averaged. As a result, we used hourly averages of H-component values for 15 stations. The average value of the hours surrounding local midnight defines the night time calm level of each night (Siddiqui et al., 2015; Soares et al., 2018). The mean magnetic field at 22:00, 23:00, 00:00, and 01:00 LT of each day is

taken as a baseline magnetic field and is subtracted from each day's data. The strength of the EEJ is, $EEJ = \Delta H_{EEJ} - \Delta H_{non-EEJ}$; where ΔH is the variation of H from the midnight mean level for a particular site. Using the difference in H between two magnetic observatories with the same longitude but different latitude, the method removes numerous sources of disturbance (Briggs, 1984). For this investigation, the monthly EEJ current variations were calculated by averaging for a minimum of 15 quiet days each month. Due to the failure of the data logger or unavailability of a minimum of 15 days magnetic data for the months in some sectors, we have used some more stations within approximately the same longitudinal zone. The results may also show the vacant in the figures if there are no magnetic data in the sector. We have also discussed it briefly in our previous work (Alemayehu & Melesew, 2022).

Table 2. List of GPS Receiver stations used in this work.

Station Name	Station Code	Geog. Lat.	Geog. Long.	Geom. Lat .	Geom. Long.
Peruvian Sector GPS Receivers Stations					
Bogota	BOGT	4.64°N	74.1°W	15.63°N	359.95°E
Huancayo	LHYO	12.1°S	75.3°W	0.14°S	357.33°E
Copiapo	COPO	27.4°S	70.3°W	15.17°S	1.13°E
Brazilian Sector GPS Receivers Stations					
Kourou	KOUR	5.3°N	53°W	8.54°N	22.09°E
Sco Luis	SALU	2.59°S	44.2°W	3.43°S	27.67°E
Brasilia	BRAZ	15.94°S	47.9°W	12.58°S	20.51°E
West African Sector GPS Receivers Stations					
Maspalomas	Mas1	27.8°N	15.6°W	19.39°N	61.06°E
CGGN	CGGN	10.12°N	9.11°E	1.49°S	83.7°E
Cotonou	BJCO	6.4°N	2.45°E	5.97°S	76.77°E
N'Koltang	NKLG	0.4°N	9.7°E	12.08°S	83.9°E
India Sector GPS Receivers Stations					
Biratnagar 2	BRN2	26.5°N	87.3°E	20.57°N	160.29°E
Pallekele	PALK	7.3°N	80.7°E	0.41°S	153.43°E
Diego Garcia	DGAV	7.3°S	72.4°E	16.13°S	143.99°E
South east Asian Sector GPS Receivers Stations					
Kunming	KUNM	25.03°N	102.8°E	18.97°N	175.66°E
Chulalongkorn	CUSV	13.7°N	100.53°E	6.68°N	173.2°E
Bakosurtanal	BAKO	6.5°S	106.84°E	15.23°S	179.24°E
Pacific Sector GPS Receivers Stations					
Minamitorishima	MCIL	24.29°N	153.97°E	17.25°N	225.2°E
U of Guam	GUUG	13.43°N	144.8°E	5.95°N	216.74°E
SA42	SA42	2.06°S	147.42°E	9.79°S	220.2°E

The RINEX observations files of TEC were processed by the GPS-TEC analysis application software, developed by Gopi Seemala (Seemala & Valladares, 2011; Ma

and Maruyama, 2003; Olwendo et al., 2016) to obtain the daily vertical TEC (VTEC) data over the stations considered in the study. The TEC values derived from GPS stations for

every month during the two years from 2011 to 2012 at all the considered locations have been used to derive the peak TEC. The altitude, occurrence of TEC peak, and the local time are the three important parameters needed to characterize the EIA crest.

3. Results

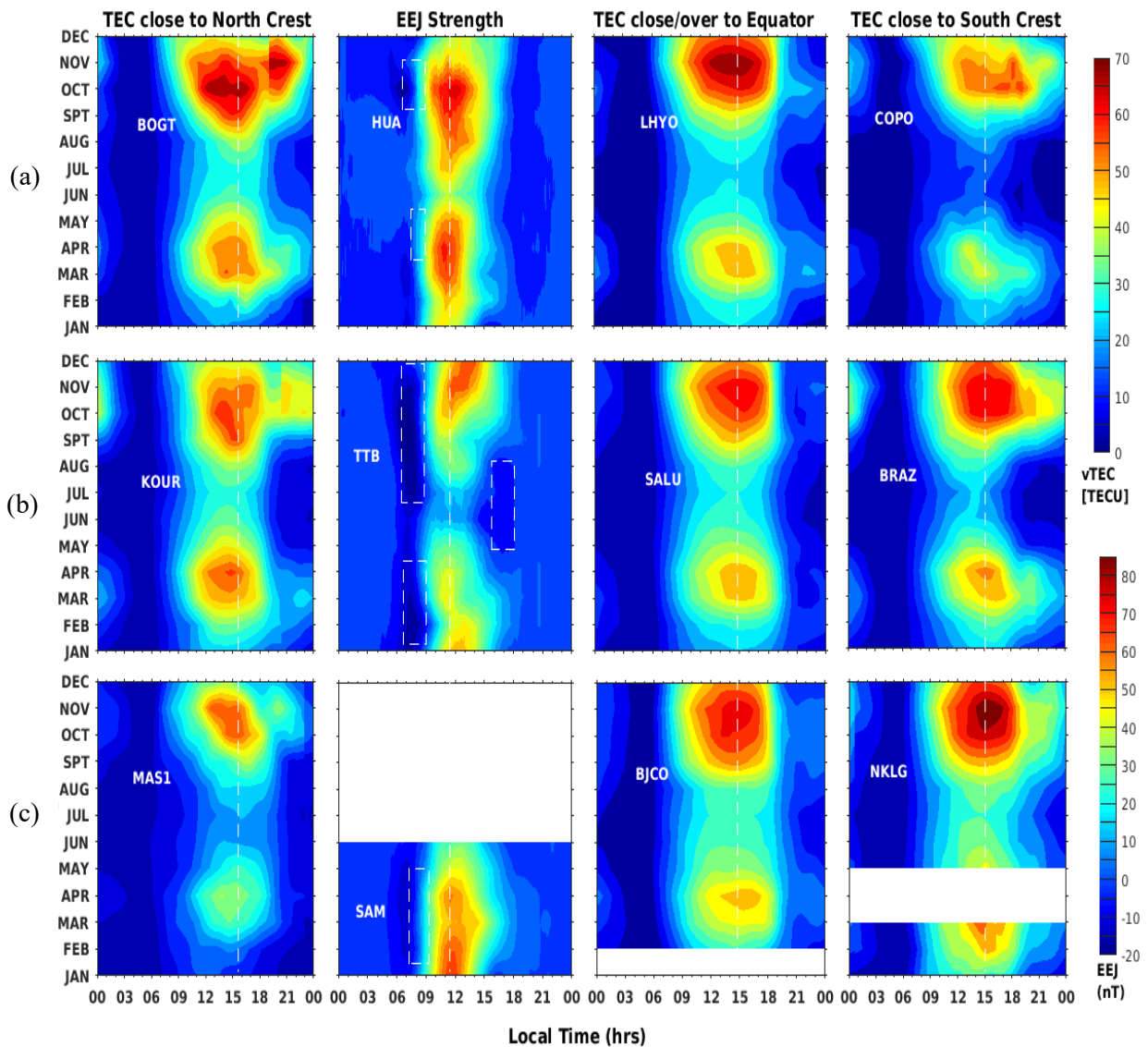
The daytime EEJ/CEJ strength and its role on the formation and development of the north/south EIA crest, equatorial trough, and the corresponding results are presented in the following sections.

3-1. Monthly diurnal variations of EEJ and TEC in different longitudinal sectors

Monthly mean diurnal variations of EEJ and its role on the TEC of EIA characteristics in the selected regions of the study during 2011-2012 are presented as contour plots in Figures 2 to 5. The second columns of Figures 2 and 3 show the monthly mean diurnal variations of EEJ values over Peruvian (Figure 2A), Brazilian (Figure 2B), West African (Figure 2C), Indian (Figure 3A), Southeast Asian (Figure 3B), and Pacific (Figure 3C) sectors during 2011. On the other hand, the first and the last columns of Figures 2 and 3 show the characteristics of northern and southern TEC of EIA crests respectively, while the third column represents the equatorial trough of TEC over those Sectors. Figures 4A to 5C show the variations of EEJ and TEC over the same sectors explained above but for the year 2012. The white spaces within a panel in Figures 2A to 5C for different months of the period of the study indicate that the stations do not have data during those months. The data gaps would limit observation of the EEJ and EIA features over the regions.

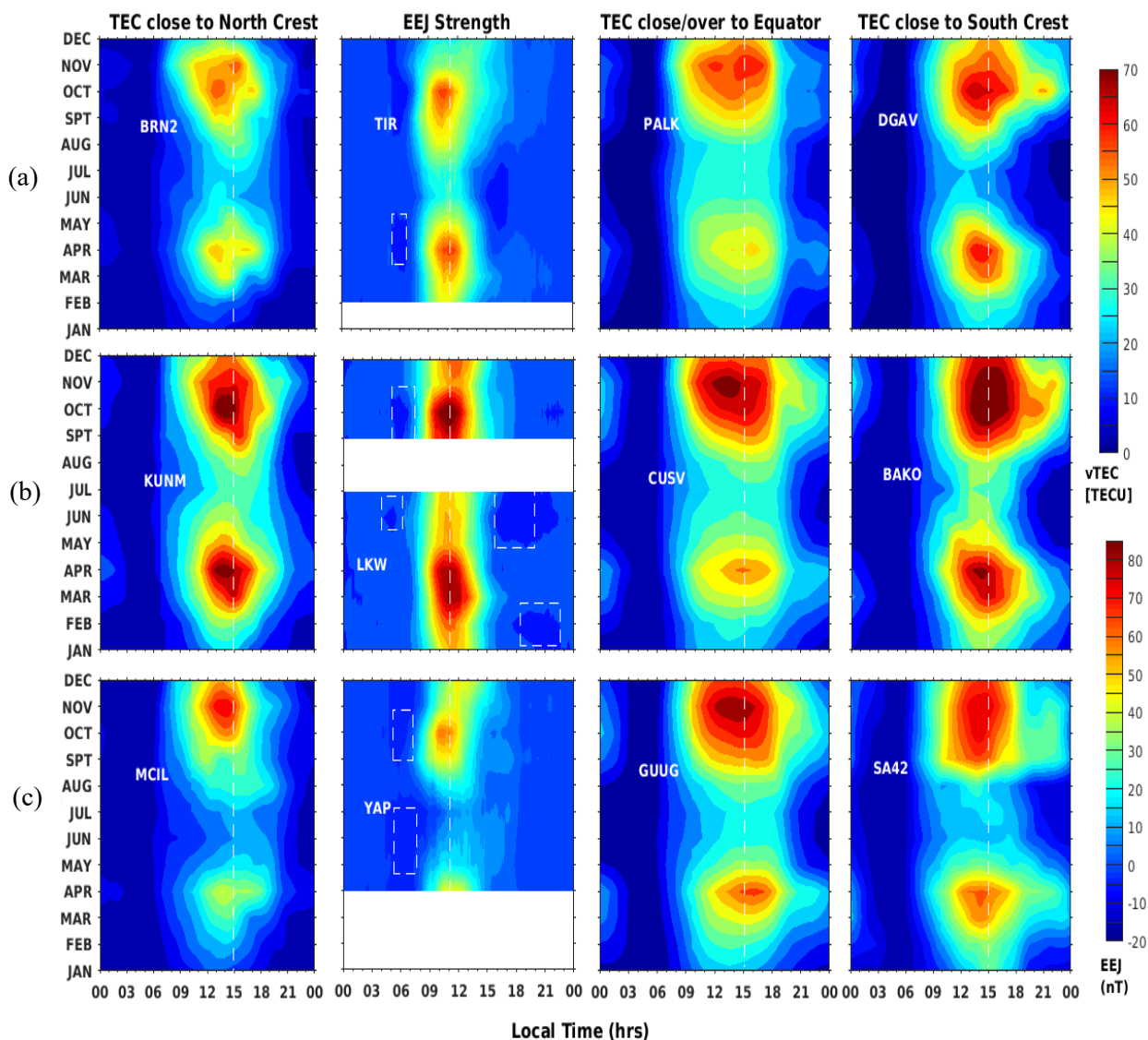
As seen from the monthly mean results in Figures 2 to 5, both EEJ and TEC have shown monthly variations with two higher amplitudes of peaks during the equinoctial months of March and September as indicated by the vertical dashed lines in Figures 2 to 5 with the maxima of the EIA crest appears roughly about four hours after that of the maximum local noontime EEJ during these

months. However, the TEC values over the equatorial/close to equatorial stations are lower compared to those over the anomaly crest locations. Figure 2A shows that the EEJ strength is near similar (almost symmetric) in both March and September equinox months over the Peruvian region. However, the hemispheric asymmetry between the northern and southern crest regions of EIA as well as equatorial trough were observed. The TEC peaks during the September equinoctial months show higher TEC peak than March equinoctial months in both hemispheres of the Peruvian and Brazilian, and West African sectors as seen in Figures 2A, 2B and 2C. The second column of Figures 2A and 2B show the occurrence of MCEJ in the Peruvian and Brazilian regions due to the westward electric fields, while the third column of Figure 2A shows the maximum TEC over the equator than the southern crest regions. It indicates that the EIA crests move closer to the equator in the Peruvian region during the winter months due to equatorward neutral winds, reversal electric fields, and the less or the zero ExB during daytime can contribute to the positive ionospheric storms observed around the equator. Balan et al. (2013) suggest that the vertical ExB drift during daytime can be zero/downward if the westward electric field (due to disturbance dynamo and/or penetration) balances/exceeds the quiet-time eastward dynamo electric field. In addition, as we can see from Figure 2C in the West African sectors, during the summer December solstice season, the northern anomaly crests shift slightly towards the equator from the north with stronger southern crests than that in June solstice. Moreover, asymmetries between the hemispheric geomagnetic fields give rise to an asymmetry in the solar radiation as well as the plasma and neutral composition that ultimately leads to hemispheric differences of the electron density in the F-region ionosphere. These contours make it clear that both EEJ and TEC have demonstrated semiannual changes, with two peaks occurring during the equinoctial months of March/April and September/October.



The 2011 EEJ and EIA variations over the Peruvian, Brazilian and West African Sectors

Figure 2. Contour plots depicting the monthly average diurnal variation of TEC close to northern anomaly crest, EEJ, TEC over/close to the equator, and TEC close to southern anomaly crest versus local time in the Peruvian (A), Brazilian (B), West African (C) sectors during the year 2011. The diurnal EIA and EEJ peaks are marked by white-dashed vertical lines. The white dot-dash rectangular boxes in the figure indicate the presence of CEJ events.



The 2011 EEJ and EIA variations over the Indian, Southeast Asian and Pacific Sectors

Figure 3. Contour plots of the daytime mean variation of EEJ and TEC strength for all quiet days of the months over the equator and North and South EIA crest locations in the Indian (panel A), Southeast Asia (panel B), and Pacific sectors (panel C) during the year 2011. The diurnal EIA and EEJ peaks are marked by white dotted vertical lines. The white dot-dash rectangular boxes in the figure indicate the presence of CEJ events, which have a great impact on the reduction of EEJ peak amplitudes in the time of occurrence of the strong CEJ days.

Figures 3A and 3B show the EEJ strengths were near similar (almost symmetric) in both March and September equinox months over the Indian and Southeast Asian regions. However, the hemispheric asymmetry between the northern and southern crest regions of EIAs was observed in those sectors. The stronger EEJ and largest TEC values with the highest variability are observed near the EIA crests in the

Southeast Asian region, thus this region is of paramount importance. As seen in Figure 3B, during local noon near the magnetic equator, EEJ reflects a strong band of eastward electric field. The results indicate that if there is a strong comparable noontime EEJ, there are well-formed late afternoon anomalous crests. These results are in agreement with the suggestions by Khadka et al. (2016).

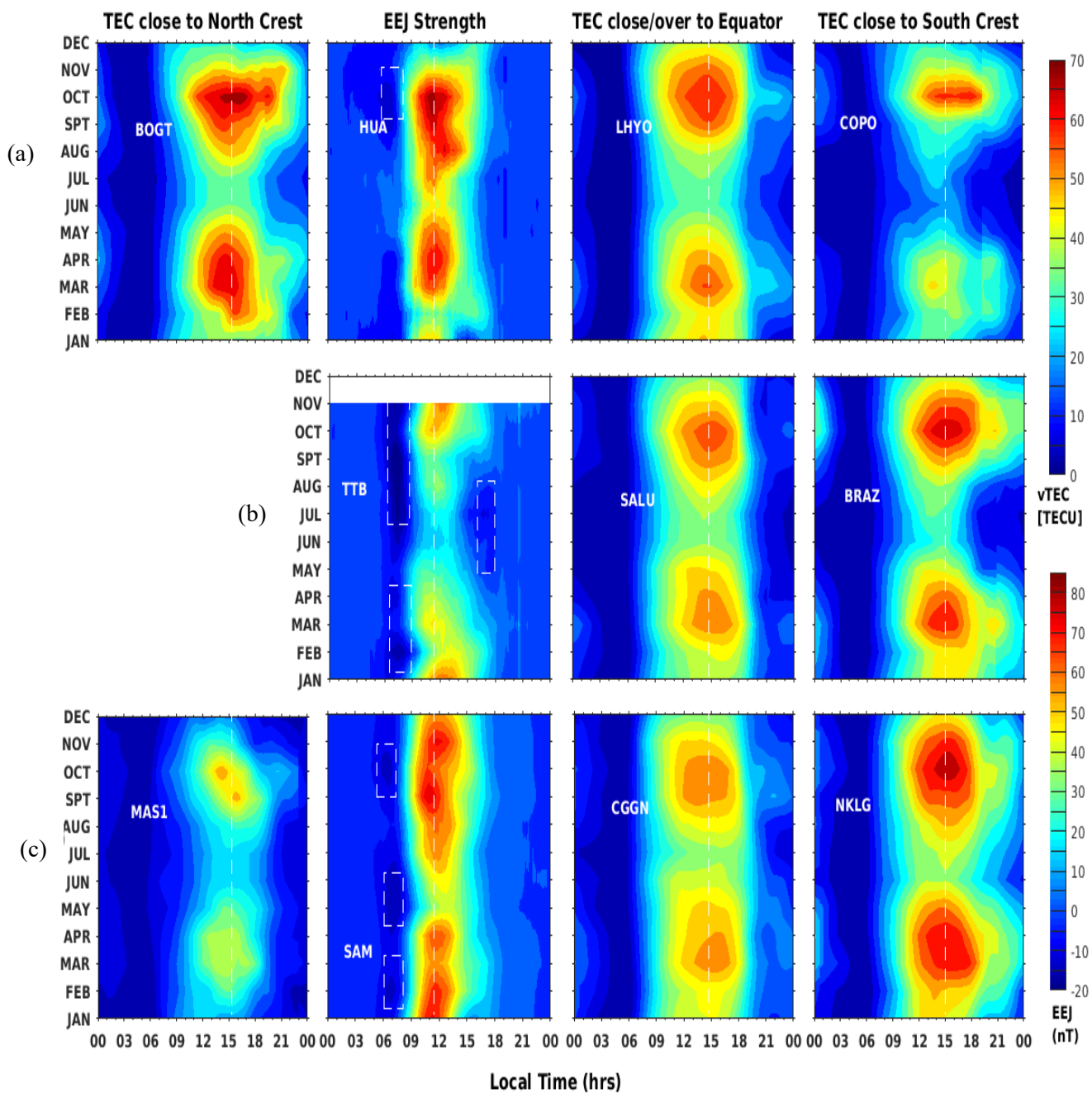
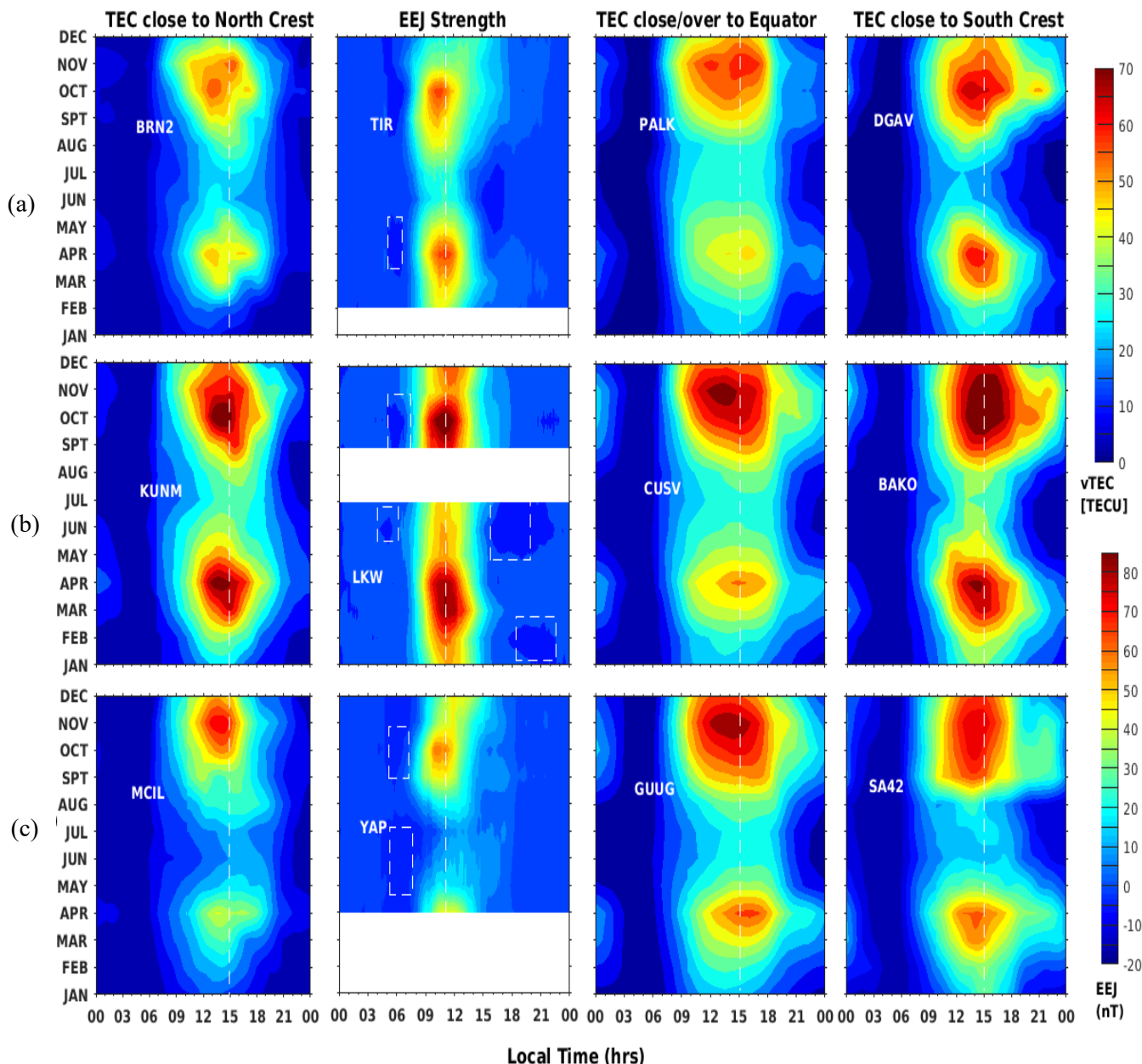


Figure 4. the same as Figure 2 but for the year 2012.



The 2011 EEJ and EIA variations over the Indian, Southeast Asian and Pacific Sectors

Figure 5. the same as Figure 3 but for the year 2012.

A double-peaked EEJ profile emerges in the Southeast Asian sector during 2012. Following these, all profiles show that two symmetric maxima TEC of EIA at about 15° north and south of the dip equator were formed at the crest regions in the sector. Additionally, the TEC semidiurnal distribution possesses a significant hemispheric asymmetry, being strong in the southern hemisphere as that in the northern hemisphere in the Indian and Pacific sectors. It can also be noticed from Figures 2 to 5 that the significant maximum in the daytime

variation of EEJ is observed from 09:30 through 14:30 LT with different strongest values that occur between around 10:00 to 13:30 LT; while the maximum diurnal variation of TEC in both the hemispheres crest and the equatorial troughs seen around 14:00 to 16:00 LT. It indicates that the two symmetrical TEC crests reach the day maximum level 3 to 4 hours later than the maximum daytime values of EEJ peak. Our study period is focused on the ascending phase of the Solar Cycle 24 (2011-2012), it is expected that the strength of EEJ and EIA are

obviously larger in equinoctial months than that in solstice months showing a clear semiannual variation. Results in our findings (–Figures 2 to 5) confirmed these and show that both northern and southern equatorial anomaly crests developed around post noon in equinoxes following the strengths of daytime EEJ peak. During these equinoctial months, the northern EIA crests are stronger in the Peruvian and Brazilian sectors than the southern one, while in the Indian and West African sectors the southern EIA crests are stronger (Figures 2 to 5).

It is seen from the contour plots in Figures 3B and 5B that both the EEJ and the intensities of northern (at KUNM) and southern (at BAKO) EIA crests are stronger in the Southeast Asian sector during the two equinoctial Months in all the years of the study (2011-2012) than June solstice months. The strength of the northern anomaly crest in the Peruvian (BOGT) is roughly higher than the southern anomaly (COPO & MAL2), while in the West African and Indian selectors, the southern (NKLG & DGAV) TEC of EIA shows relatively the highest. Moderate and approximately equal peaks of north/south (KOUR/BRAZ) EIA formations are observed in the Brazilian sector. The weak EEJ monthly peak and roughly weak but equal formations of north/south EIA are observed in the Pacific sector during equinoctial months from the year 2011 to 2012. The equatorial troughs are more pronounced during March equinoctial months at the Brazilian (SALU), West African (CGGN/BJCO), Indian (PALK), Southeast Asian (CUSV), and Pacific sectors (GUUG). However, most of the ionization is observed over the equator during September equinoctial months in the Peruvian (LHYO) and Brazilian (SALU) as noted in the results from the GPS observations (Figures 2 to 5). A reason for the phenomenon is that the solar dependence of the afternoon zonal electric field is in the ionospheric F region (Huang et al., 2013). The same situations are observed in the Southeast Asian (CUSV) and Pacific sectors (GUUG) during moderated solar activity period 2011.

Furthermore, during 2012, weak EEJ but strong anomaly crests are observed in the Brazilian sector (Figure 4B). This indicates that the photochemical processes due to the

varying solar intensity also have a great role for the formation of EIA in the Brazilian sector, in addition to the combined effect of the geometry of the geographic and geomagnetic equators and the solar zenith angle (photoionization) (Dias et al., 2020). The conditions of solar activity also have a marked effect on the north–south asymmetry of the EIA (Huang et al., 2013, 2014). Figure 4c shows the strong and relatively symmetric monthly mean EEJ and weak northern but strong southern peaks of EIA in the West African sector. The north and south peaks of the EIA have asymmetries during summer or winter solstice due to the nature of the resulting meridional neutral winds in the F-region. Figure 5 represents the EEJ variations and its effect on TEC anomaly crest in the same location as described in Figure 3 but for the year 2012. During the June solstitial months (May-August) in all sectors in this study (Figures 2 to 5), the GPS-TEC shows a very weak anomaly, and could not reach up to 15° to 20° dip latitudes, and most of the plasma is confined over the geomagnetic equator, while the intermediate TEC values are noted during the December solstitial months (November, December, January), exhibiting moderate EIA anomaly.

3-2. The Statistical description of EEJ, MCEJ/ECEJ and EIA

The day-to-day variability of EIA and the characteristic features of the EIA exhibit strong dependence with the EEJ diurnal characteristics (Huang et al., 1989; Chen et al., 2008; Venkatesh et al., 2014; Mo et al., 2018). To confirm this, Figure 6 shows the relation between the daytime EEJ/CEJ strength with the TEC close to EIAs crests with the bar graphs; each graph represents the rate of average peaks of parameters at each sectors. The % longitudinal inequality of EEJ, % difference of northern/southern TEC of EIA, equatorial TEC of trough, % occurrence of MCEJ, and ECEJ in different months along the magnetic dip equator over the period of study are examined and presented in the form of bar graphs in Figure 6. According to the amplitude of EEJ, TEC, and the time of occurrence of the MCEJ/ECEJ, the bar graphs are divided into three subsections.

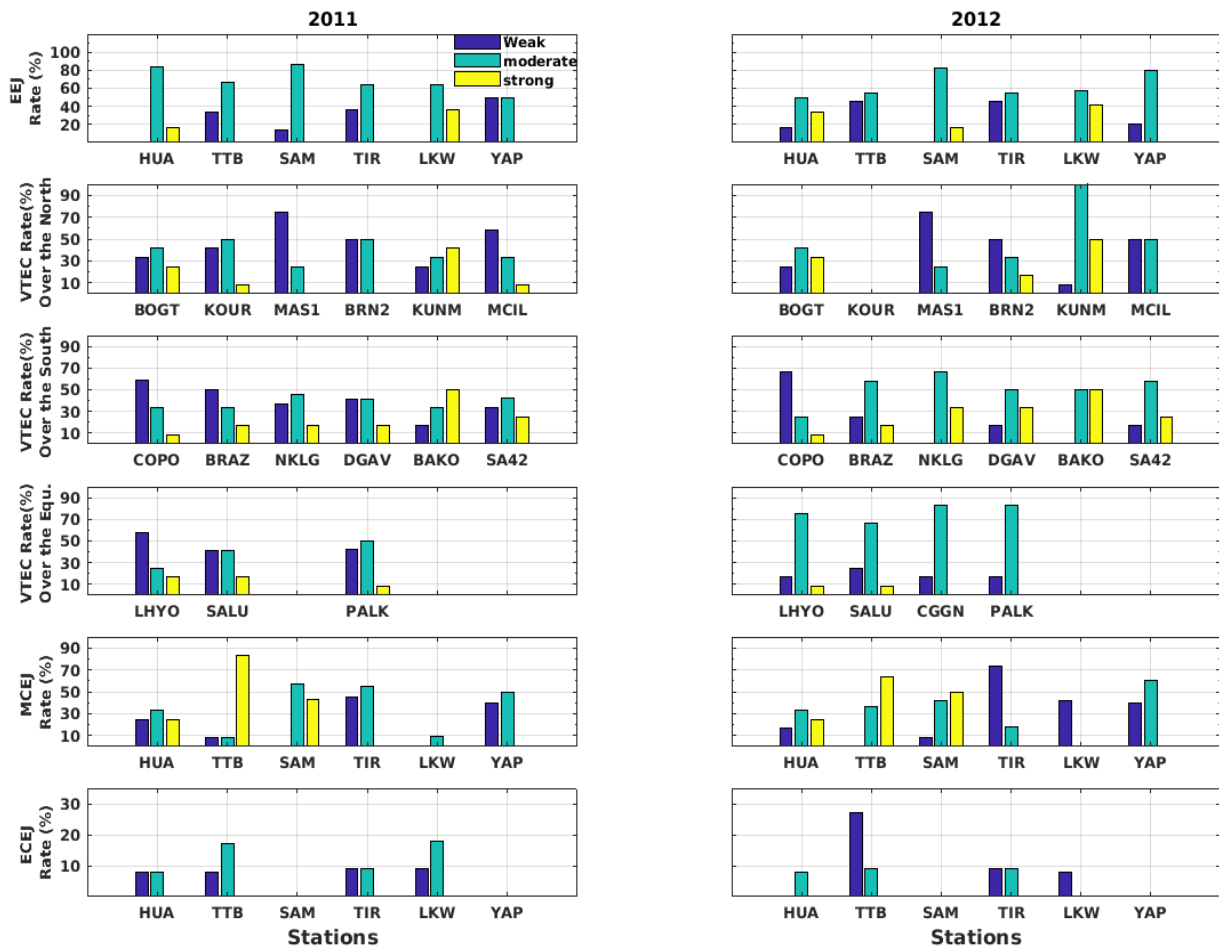


Figure 6. Histograms exhibiting the classification of the longitudinal variability of the monthly mean EEJ rates (first row (panels)), northern and southern TEC of EIA rates (second and third rows (panels)), equatorial TEC of trough rate (fourth row (panels)), the occurrences of total morning counter electrojet (MCEJ fifth row panels) rates, and the occurrences of total evening counter electrojet (ECEJ sixth row (panels)) rates computed from the ground-based data in the years between 2011 and 2012, obtained from the monthly plots (Figures 2 to 5).

The EEJ amplitudes are classified as weak (40 nT), moderate (≥ 40 to 70 nT), and strong (≥ 70 nT), while the TEC amplitudes are likewise divided into three categories: weak (40 TECU), moderate (≥ 40 to 60 TECU), and strong (≥ 60 TECU). Following the methodology of Chandrasekhar et al. (2014), Rabiou et al. (2017), Soares et al. (2018), Alemayehu & Melesew (2022) and using defined local time (LT) intervals for the occurrence of MCEJ (06:00 to 10:00 LT) and ECEJ (15:00 to 18:00 LT), we have calculated the MCEJ and classified its strength into three categories such as. (i) ≤ -2 to > -4 nT (weak), (ii) < -4 to ≥ -8 nT (moderate), and (iii) < -8 nT (strong). As shown in Figure 6, the prevalence of ECEJ at TTB has risen from weak/moderate in 2011 to moderate/strongest in 2012. According to Guizelli et al. (2013), the frequency of EEJ

deviations varies depending on the season, with varying levels of events. They claim that there is a 25% chance of anomaly developing after 06:30 LT, and that the deviations over Jicamarca reach their maximum values between 07:30 and 1100 LT, especially during the equinoxes season. Our findings in Figure 6 support their assertions. Moreover, as we can see in Figure 6 (fourth, fifth and sixth panels), the percentage of monthly mean of TEC at the equatorial trough shown strong, moderate and weak rate during strong CEJ rates in the Peruvian, Brazilian and West African sectors. Due to the reversal of electric field (lowering the EEJ peaks), it may imply poor supply of plasma to the crest location resulting in larger probability and amplitude of decrease in TEC on the days of CEJ events.

It is seen from these bar graphs in Figure 6

that the percentages of monthly mean of daytime EEJ in most of the Peruvian, Southeast Asian and West African sectors showing the strongest and moderate rates. For example, the rate of EEJ across the Peruvian sector is 18% in 2011 and 35 % in 2012 strongest, while it is 38% in 2011 and 42% in 2012 strongest across the Southeast Asian sector, and 85% moderate in 2011 and 18% in 2012 strongest over the West African sector. Observations from the bar-graph in Figure 6 also that the monthly rate of TEC in the northern region of the Peruvian sector (BOGT: 25% in 2011 & 33% in 2012), the Southeast Asian sector (KUNM: 42% in 2011 & 50% in 2012), and West African sectors witnessed strongest rate. The monthly mean of TEC in the northern zone of the Brazilian (except unavailability of data in 2012), and Indian sectors showing an increment rate from the year 2011 to 2012. It is noted in the first, second, and third rows of Figure 6 that the percentage of EEJ in the Peruvian (HUA) and Southeast Asian (LKW) sectors with corresponding north and south TEC of EIA shows the highest rate and it increases gradually from the year 2011 to 2012. The percentages of the daytime EEJ in the Indian (TIR), and Pacific (YAP) sectors show a weak and moderate rate, while the corresponding rate of TEC in those sectors shows the weak, moderate, and strongest percentages. However, in the Brazilian (TTB) and African (SAM) sectors, the percentages of EEJ show a weak and moderate rate, while the corresponding rate of TEC of EIA and the occurrence rate of MCEJ in those sectors shows roughly the strongest.

When the maximum rate of CEJ is recorded at the station, the EEJ has a lower peak, as shown in Figure 6. The percentage of EEJ and CEJ varies from one longitudinal to the next, with the highest rate of EEJ in the Peruvian and Southeast Asian sectors and the highest rate of monthly CEJ in the Brazilian sectors, as shown in Figure 6. The evening CEJ events are also demonstrated to be quite fugacious from one longitude to another (Figure 6). The Peruvian, Brazilian and West African sectors have consistently higher monthly MCEJ occurrence rates than the other sectors (Figure 6). The Indian and Southeast Asian as well as Pacific sectors have shown the lowest and moderate

percentage of the MCEJ. These relationships lead us to conclude that an EIA can also arise during weak Counter Electrojets (CEJs). For the case of low EEJ strength (<40 nT) at East Brazilian, African, Indian and Pacific sectors, the overall occurrence of the southern GPS-TEC rate shows the weak, moderate, and strongest rate as noted in the third row of Figure 8. The overall occurrence of averages monthly TEC of EIA in the dip equator LHYO (0.14°S,357.33°E) and the edge of the dip equator PTAG (7.61°N,193.42°E) is showing the strongest and ascending rate from the year 2011 to 2012. Stolle et al. (2008) also indicated that the TEC of EIA can develop during weak Counter Electrojets (CEJ). The moderated ECEJ also pronounced in the Peruvian, Brazilian and Indian sectors during 2011 and 2012. The EEJ strength is influenced not only by the zonal electric field, but also by the electron density in the lower ionospheric F zone, which may have a well correlated with solar EUV flux. Mo et al. 2018 also suggested that the diurnal, seasonal, and solar activity variations of EIA crest are consistent with that of the strength of equatorial electrojet. We mainly focused on the longitudinal variations of EEJ and its effect on the variations TEC during the ascending phase of Solar cycle 24. In the future, it is to be important to study the correlations between the seasonal dependence of EEJ and its effect on the TEC and location of EIA crest with the solar EUV flux across the globe during the solar maximum years. As it clearly seen from the figure that there is a good correlation between the EEJ strength and TEC magnitudes.

3-3. The relationship between EEJ and TEC at different longitudinal sector

As described in the introduction, the driving force behind the fountain effect creating the EIA is the $E \times B$ drifts over the equator being controlled by the strength of the EEJ (Venkatesh et al., 2014). As the daytime EEJ strength increases, the upward electrodynamic drift velocity increases; this causes plasma to move to higher altitudes, and as a result, the anomaly crests move to a higher latitude (Huang et al.; 1989, Mo & Zhang, 2021). Chen et al. (2013), Venkatesh et al. (2014), Mo et al. (2018) indicated that

the day-to-day variability of EIA and the characteristic features of the EIA exhibit strong dependence with the EEJ diurnal characteristics. To confirm this, Figures 7 to 9 show the correlation of the TEC close to EIAs crests/over the equator versus the daytime peak EEJ (day_maxEEJs) and afternoon CEJ strength in the Peruvian and Brazilian sectors (in which the CEJ events were more pronounced) and the Southeast Asian region that has low or weak CEJs event. Each dot represents the daily average peaks of these parameters.

The correlation coefficient (CC) between the northern crest region TECs (over the equator TECs) and day_maxEEJs over the Peruvian region are 0.57 (0.39) and 0.51 (0.6) for the years 2011 and 2012 respectively, whereas the corresponding coefficient of determinations were 33(15)% and 26(36)%. On the other hand, the southern zone (close to the equator) of the Brazilian sector, the CCs are 0.6(0.44) and 0.4(0.11) with the corresponding coefficient of determinations 36(19)% and 16(1)% for the years 2011 and 2012 respectively, as shown in Figure 8. This figure indicates that in the Peruvian around northern and Brazilian sector around southern crest regions, different rate of the variability of TEC is accounted for by the variability of day_maxEEJs . On the other hand, in the Southeast Asian sector, 38% and 36% of the variations of TEC in the northern region are due to the variations of day_maxEEJs during 2011 and 2012 respectively, while 25% and 18% of the variability of TEC close to southern EIA crest are due to the variation of day_maxEEJs during 2011 and 2012 respectively (see Figure 9). Both these plots (Figures 8 and 9) indicate that there exists a positive dependency of the TEC of EIA strength on the strengths of EEJ parameter. It is seen that the scatter between TEC of EIA strength and EEJ daymax is greater in the northern region compared to those between EIA strength and EEJ daymax values in the southern region at the selected sectors among the investigated sectors in our study.

To understand the effect of the day_maxEEJs

on the strength of the EIA crest, some examples of the EIA along with the corresponding EEJ diurnal variations over Peruvian, Brazilian and Southeast Asian sectors have been plotted and presented in Figures 8 and 9. However, the peak of day time EEJ might be reduced by the occurrences of morning equatorial electrojet (MCEJ) as we have already presented in our previous paper (Alemayehu & Melessew, 2022). As we have tried to show in Figure 10, there is less/weak direct effect of MCEJ on the formation/collapse of EIA. Nevertheless, it is very interesting to note that the CEJ events in the afternoon may have contributions to the inhibition of TEC from propagating it to close to the northern/southern crests as we can see in Figure 11. The results at Peruvian and Brazilian are thus similar to those at other longitudes studied earlier (Basu et al., 2009). In the southeast Asian sectors with weak/null CEJs events, day_maxEEJs gives strong support to the formation of the clear anomaly with a strong EIA crest (Figure 3, Figure 5, and Figure 9). The morning CEJ and afternoon CEJ occurrence peaks for TTB and HUA were calculated from each quiet day values correlated them with the corresponding day maximum TEC values in the same latitude, for the period from January 2011 to December 2012, as shown in Figures 10 and 11 for day max TEC with day max MCEJ and TEC with ACEJ.

Scatter plots between the EEJ daymax and the aforementioned TEC strength at different locations (TEC at the northern EIA crest, TEC over to the equator) the first and the second panels have been plotted for the Peruvian sector while the third and the fourth panels represent the TEC at the southern EIA crest and TEC close to the equator in the Brazilian sectors and presented in Figure 7. R indicates the value of correlation coefficient, while the values of R^2 represent the contribution of the EEJ on the formation and the variation of EIA. Additionally, the plots and linear correlations between both parameters, peak TEC variation and day_maxEEJ , are shown in Figures 7 to 10.

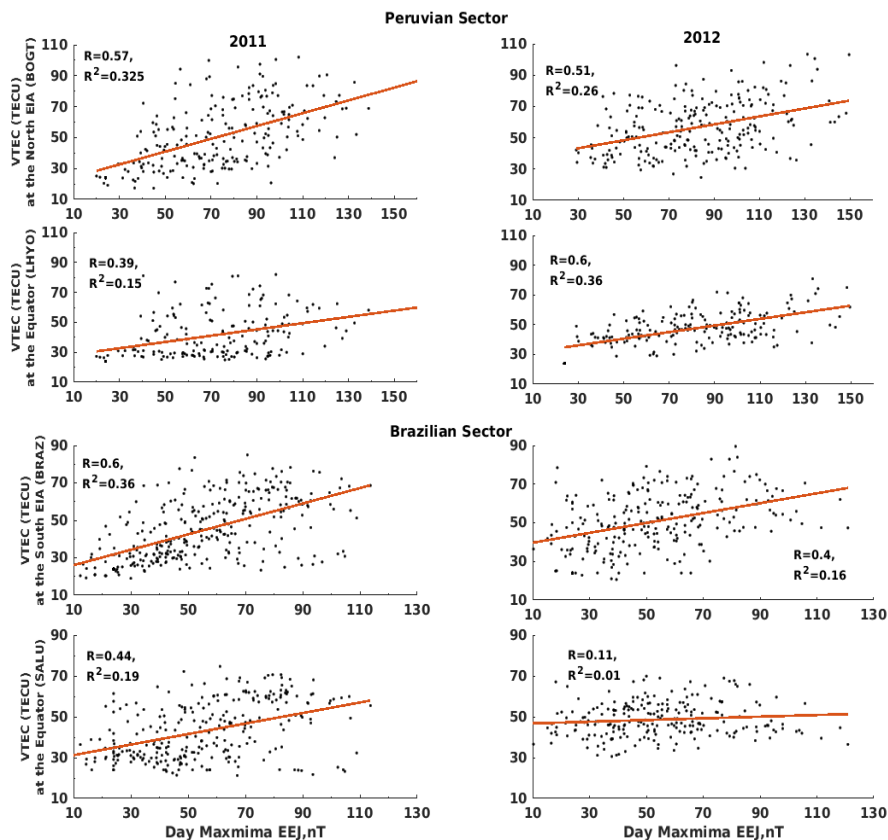


Figure 7. Scatter plot showing the correlation of the variations of the TEC at the close to northern/southern EIA crests and TEC close/over the equator versus the monthly averages of EEJ and integrated VTEC within the same longitude over the Peruvian and Brazilian sector during 2011 to 2012.

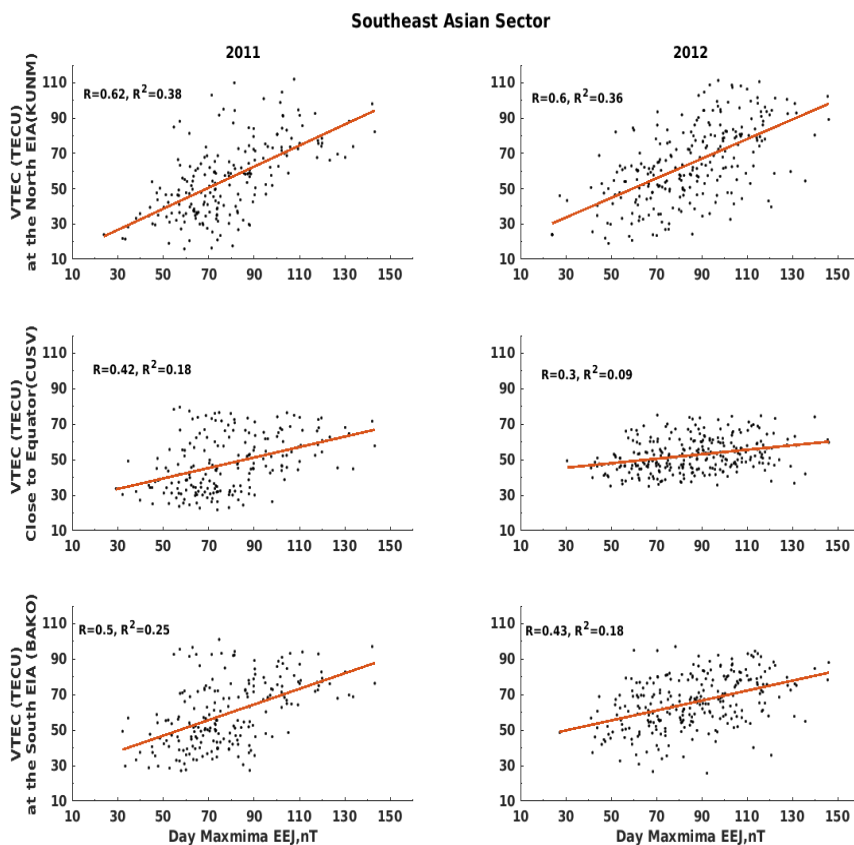


Figure 8. The same as Figure 7 but for Southeast Asian Sector.

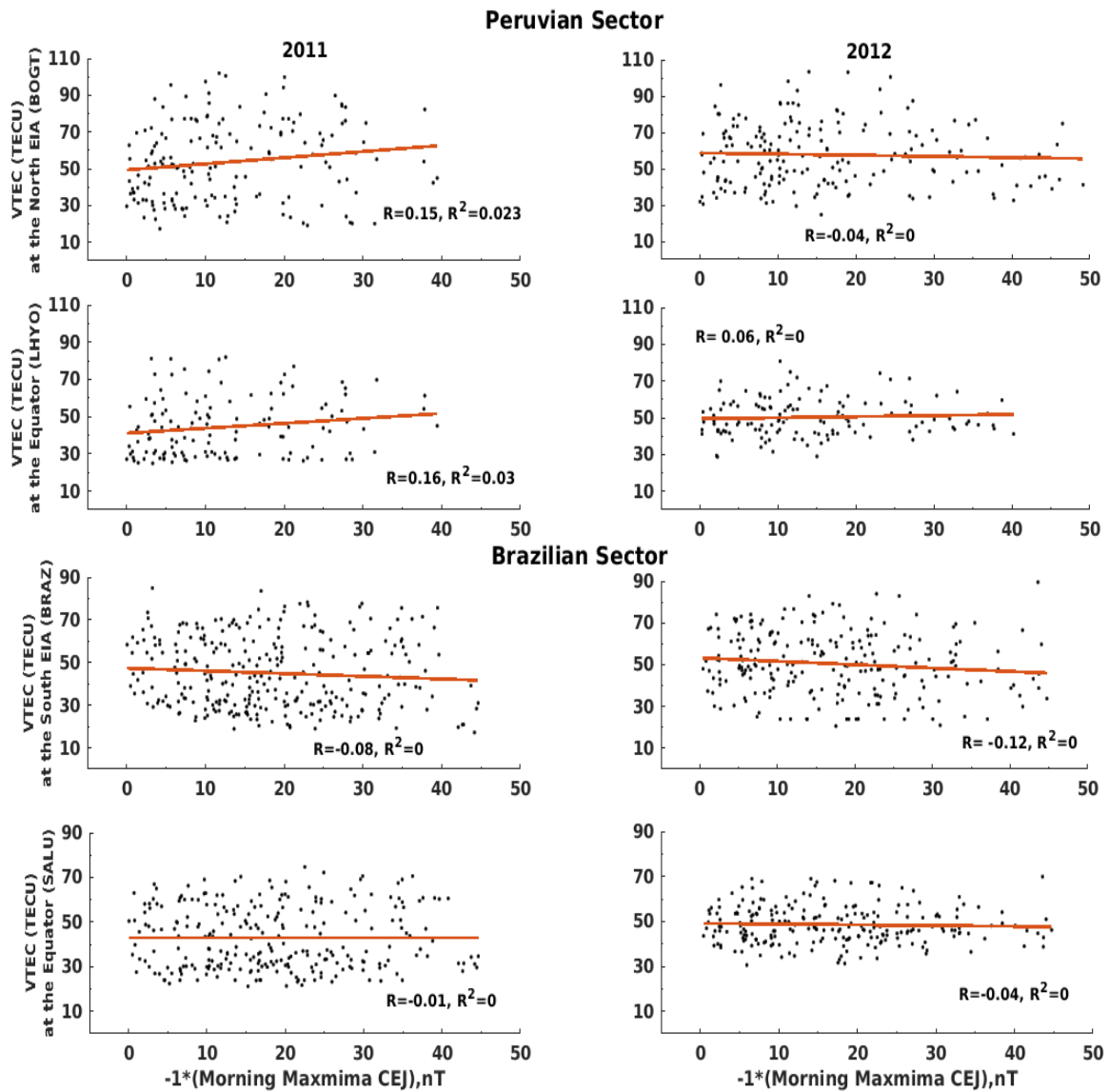


Figure 9. Scatter plot showing the correlation of the variations of the monthly averages of TEC at the close to EIA crests (TEC over or close to the equator) versus the day maximum of MCEJ within the same longitude over the Peruvian sector (panel 1 and panel 2) and Brazilian sector (panel 3 and panel 4) during the years 2011 to 2012.

All the panels of Figure 9 show weak correlation of EIA and the occurrence of MCEJ.

However, the results of our findings in Figure 10 clearly indicate the collapse of the EIA peaks, when a CEJ event was present a few hours earlier in the Peruvian

and Brazilian sectors. Perhaps this result provides some evidence for the unexplained positive relationship between the strength of the EEJ during the daytime and the strengths of EIA; and negative relations of afternoon CEJ with TEC strengths.

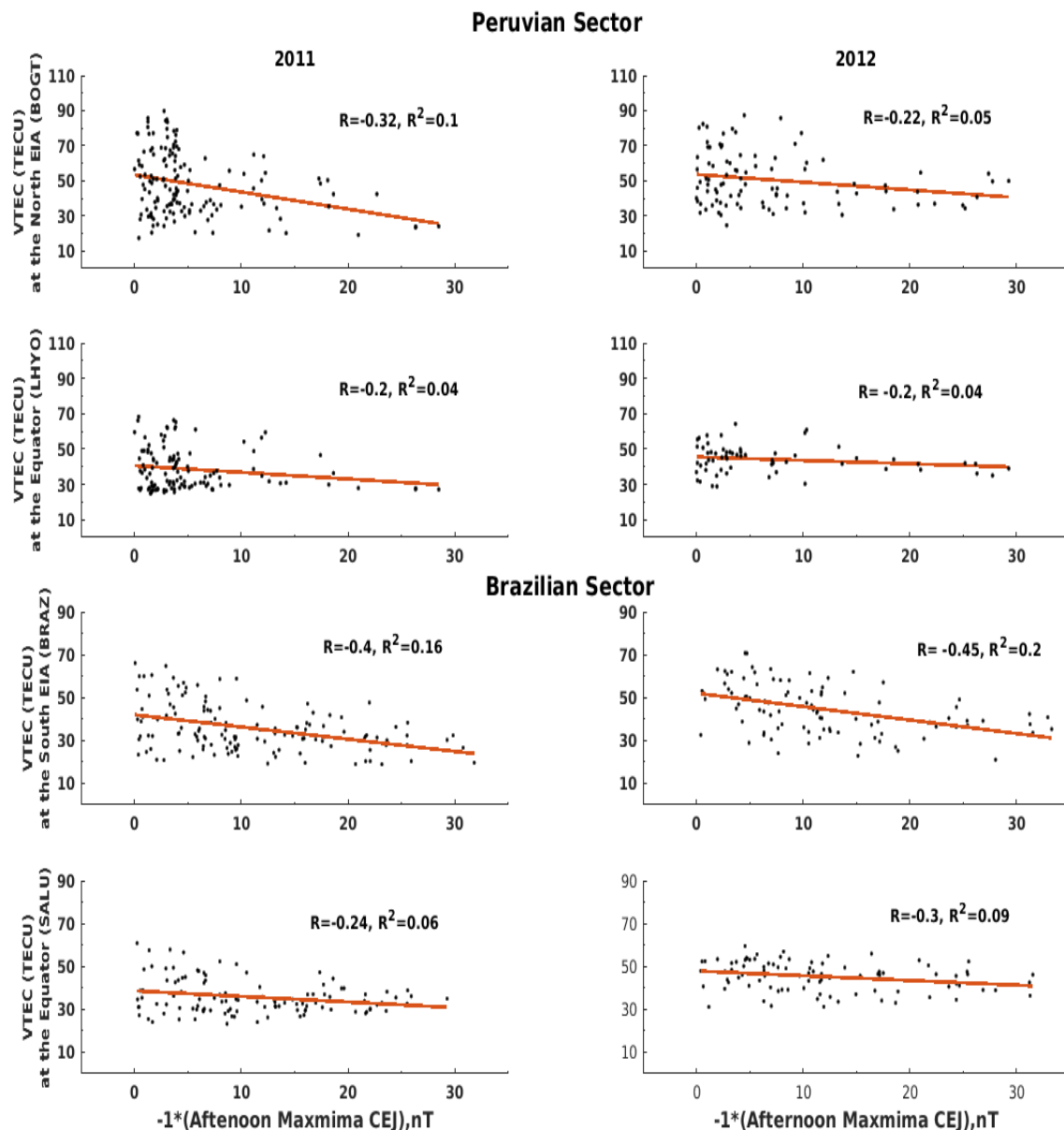


Figure 10. Scatter plot showing the correlation of the variations of the monthly averages of TEC at the close to EIA crests (TEC over or close to the equator) versus the day maximum of ACEJ within the same longitude over the Peruvian sector (panel 1 and panel 2) and Brazilian sector (panel 3 and panel 4) during the years 2011 to 2012.

4. Discussion and Conclusions

In this study, we have studied the comprehensive comparison of the longitudinal and monthly mean variabilities of EEJ and its role on the diurnal characteristics of the north-south asymmetry of the equatorial ionization anomaly (EIA), and equatorial trough during quiet time from 2011 to 2012 across the six equatorial-low-latitude longitudinal sectors. The magnetometer measurements from the eight paired dip-equatorial stations over the

Peruvian, Brazilian, West African, Indian, Southeast Asian and Pacific sectors during the increasing phase of the solar activity years 2011-2012 are used to derive the EEJ values. Investigation into the EEJ from six pairs of equatorial magnetic stations and TEC from 23 GPS stations (from three different chains of GPS station along the common meridian of EEJ station) has been carried out to understand the role of EEJ on the EIA characteristics in the selected regions. The amplitude of the eastward current EEJ and

EIA crests depend on the seasons, being highest in March and September equinox months for all the years from 2011 to 2012 and increases the peaks from year to year. It is noted that, as the EEJ has a higher magnitude in equinox months than solstice months, the similar diurnal variation can be seen in TEC of EIA also. The pattern of variability and longitudinal trend, significant differences separation of EEJ at 75°W, 48°W, 5°W, 77°E, 105°E, and 138°E with the chains of GPS-TEC of EIA covering a geomagnetic latitude range of 15°S to 15°N observed in daily, monthly averages and seasonal trends are being reported for the first time. Figures 2 and 4 show examples of a weak EEJ profile and a large CEJ profile (Figures 2B and 4B), with associated TEC maps for the day. The double-crest structure barely formed as the EEJ intensity was relatively weak, while the CEJ resulted in a single peak at the equator, meaning that the EIA was inhibited completely. Our results are in agreement with the suggestions by Hajra et al. (2009) and Wan et al. (2022).

The present study demonstrates that the mean monthly and seasonal diurnal variability of TEC and the characteristic features of the EIA crest and equatorial trough exhibit strong dependence on the average daytime EEJ characteristics. It is observed in Figures 2 to 5 that there are well-formed afternoon EIA crests around 15:00hLT at $\sim\pm 15^\circ$ dip latitudes especially during equinoctial months if there is a strong corresponding local noontime EEJ. Thus, the longitudinal variations in EEJ and its effect on TEC of EIA are perceivable in daily as well as monthly-averaged values. In other words, during high solar activity, there may be another mechanism ruling the TEC over selected stations besides the EEJ. This fact reinforces the conclusion that another mechanism may role the ionosphere dynamics during higher solar activity. The higher amplitudes of EEJ at HUA, LKW, followed by SAM as well as north/south EIA crests during the equinoctial months are consistent throughout observation period (Figures 2 to 5), while consistencies of the moderate and weak amplitudes in June/December solstice months. Due to strengths of day time EEJ and weak CEJ, the strength of north/south anomaly crest (peak TEC at the EIA crest) is well represented by

GPS observations during the two symmetrical equinox months of the whole period of the study at Southeast Asia (KUNM & BAKO) sectors, which have shown the semiannual behavior with two peaks in the equinoctial months.

Therefore, a simultaneous study of the monthly, as well as seasonal characteristics of EEJ and EIA, is useful in understanding the quantitative role of EEJ on the equatorial and low-latitude ionospheric plasma density variabilities over Peruvian, Brazilian, African, Indian, Southeast Asian and Pacific. Although many studies have been carried out, the variation of EEJ effects on northern and southern anomaly crests along the six longitudinal sectors during the quietest periods have not been simultaneously studied by using ground-based data. This will be helpful to improve our understanding of EEJ strength roles in the formation of fountain effect and in achieving improved accuracy in the estimation of equatorial and low-latitude ionospheric total electron content (TEC) and corresponding range delays required for the satellite-based communication and navigation applications. The results (Figures 2 to 5) clearly show that high EEJ strength occur simultaneously with the prominent EIA in most sectors of the investigations especially in the Southeast Asian sector followed by Peruvian sectors and West African sectors. This suggests that the equatorial electric field and the magnitude of the background magnetic field are also stronger in those sectors than in the other sectors. Consequently, the vertical drift should be stronger in the Peruvian sector and the Southeast Asian sectors, and more plasma should be transported to the EIA region in these sectors (Liu et al., 2001). The results of this study are consistent with the previous study by Stolle et al. (2008), Chen et al. (2008), Hajra et al. (2009), Ghosh et al. (2020). Additionally, the variation of TEC of EIA crests may also be caused by changes in the production and loss rates of electrons in the ionosphere Mo et al. (2018). Therefore, we may suggest that the daytime maximum of the EEJ is relatively more influential for the formation of north/south EIA than other parameters like EUV flux and neutral composition during moderate and low solar cycle activities.

During the rising periods of the solar cycle variation, the changes of neutral winds and neutral compositions in ionospheric height increase the O/N^2 ratio and lead to a greater production rate of ionization as the EUV flux increases.

The equatorward motions and significant TEC decreases of the equatorial anomaly crest suggest that an upward electric field near the epicenter and/or the equatorward neutral wind in the ionosphere play important roles (Liu et al., 2001). The reversal of the electric field causes downward drift motion at the equator and the moment of ionization to the latitude range of 15° - 20° becomes ineffective (Deshpande et al., 1977). Deshpande et al. (1977) and Stolle et al. (2008) have also indicated that short-lived EIA on a day with a Counter Electrojet (CEJ) in the afternoon, and the absence of the EIA on a day when no electrojet developed. The presence of CEJ during quiet days suggests the foremost role of driving EEJ current over the equator in the alterations of spatio-temporal distributions of TEC over the low latitude region (Talari & Panda 2019). These are also the causes that TEC over the equator is higher than the TEC at northern/southern crests (in the Peruvian, Brazilian African sectors). On the days of CEJ events, the diurnal variations of TEC exhibit deviations (decreases) from monthly mean values, but the feature is not regular throughout the observing period. Our results also seem to exhibit significant association with TEC decreases on the days of CEJ events. However, an EIA in TEC develops during weak CEJs are observed in the Brazilian sectors. Jonah et al. (2015) indicated that the TEC values at the EIA crest during winter across the South American sector are lower than at equatorial regions. This is because the solar radiation time during winter is weaker than summer and equinox, and the fountain effect is not strong enough to transport the plasma from equator to low latitudes in addition to the meridional or zonal winds could be important to explain the changes in TEC. These studies may have a great role in the more accurate prediction of range delays and total electron content (TEC) needed for satellite-based communication and navigation applications. In general, the

Northern/Southern TEC of EIA crests experience an increase and decrease process with the daytime variation of EEJ strength. The seasonal variations of EIA crest are consistent with that of the strength of equatorial electrojet (EEJ). The correlation coefficients of the EIA with EEJ strength are relatively high during moderate year 2011 across all sectors.

As we can see in results (–Figures 7 to 10) the strength of the EIA has shown relatively good correlation with the day maximum EEJ. In Figures 7 to 10, that is, considering to the mean peak TEC versus day_maxEEJ, relatively a higher correlation was found in 2011 compared to the year 2012, indicating that the TEC variation was caused by the effect of day time EEJ in addition to solar flux other parameters. This is in agreement with Romero-Hernandez et al. (2018) and Vaishnav et al. (2020). It is well known that during high solar activity, weak correlations are observed compared to the moderate solar activity conditions. In other words, during high solar activity, there may be another mechanism ruling the TEC over selected stations beside the EEJ. This fact reinforces the conclusion that another mechanism may role the ionosphere dynamics during higher solar activity.

Acknowledgments

This work was done at the Department of Physics, CNCS, Institute of Geophysics Space Science and Astronomy, Addis Ababa University, Ethiopia. The authors are thankful to them. We thankful and gratefully acknowledge the following data sources and their staffs for the opportunity to access the ground magnetometer data. The datasets generated during and/or analyzed during this study are available in the following links. The data for this study were downloaded from Low-latitude Ionospheric Sensor Network LISN: <http://lisn.igp.gob.pe/data/> for PIU & LET stations, from the INTERMAGNET data center: <https://www.intermagnet.org/index-eng.php> for AAE, HUA, KOU, TAM, ABG & GUA Stations, from AMBER Network: <http://magnetometers.bc.edu/index.php/amber2> for ETH station, from the Bureau Centrale de Magntisme Terrestre BCMT Network:

<http://www.bcmf.fr/wamnetnetwork.html>) for the SAM station, from WDC Catalogue (the World Data Centre (WDC) for Geomagnetism, Edinburgh):<http://www.wdc.bgs.ac.uk/dataportal/>. TTB & QGZ station, and from SuperMAG website: <http://supermag.jhuapl.edu/> for TIR, BCL, LKW & KTB stations. The authors wish to express their sincere thanks to UNAVCO (<https://www.unavco.org/data/gps-gnss/data-access-methods/data-access-methods.html>), to CDDIS Archive Explorer (https://cdis.nasa.gov/Data_and_Derived_Products/CdisArchiveExplorer.html), and (LISN) <http://lisn.igp.gob.pe/data/> teams for the GPS-TEC data resources they made available to the public.

References

- Abdu, M.A., Ramkumar, T.K., Batista, I.S., Brum, C.G.M., Takahashi, H., Reinisch, B.W., & Sobral, J. H.A. (2006). Planetary wave signatures in the equatorial atmosphere-ionosphere system, and mesosphere- E- and F-region coupling. *J. Atmospheric and Solar-Terrestrial Physics*, 68, 509–522. <https://doi.org/10.1016/j.jastp.2005.03.019>.
- Cherkos, A. M., & Nigussie, M. (2022). A study of spatio-temporal variability of equatorial electrojet using long-term ground-observations. *J. Adv. Space Res.*, 69(2), 869–888. <https://doi.org/10.1016/j.asr.2021.10.014>.
- Anderson, D., Anghel, A., Yumoto, K., Ishitsuka, M., & Kudeki, E. (2002). Estimating daytime vertical ExB drift velocities in the equatorial F-region using ground-based magnetometer observations. *Geophysical Research Letters*, 29(12), 37–1–37–4. <https://doi.org/10.1029/2001GL014562>.
- Anderson, D., Anghel, A., Chau, J., & Veliz, O. (2004). Daytime vertical ExB drift velocities inferred from ground-based magnetometer observations at low latitudes. *J. Space Weather*, 2(11), <https://doi.org/10.1029/2004SW000095>.
- Anderson, D., Anghel, A., Chau, J., Yumoto, K., Bhattacharyya, A., & Alex, S. (2006). Daytime, low latitude, vertical ExB drift velocities, inferred from ground-based magnetometer observations in the Peruvian, Philippine and Indian longitude sectors under quiet and disturbed conditions; ILWS WORKSHOP 2006, GOA (2006).
- Bagiya, M. S., Joshi, H. P., Iyer, K. N., Aggarwal, M., Ravindran, S., & Pathan, B. M. (2009). TEC variations during low solar activity period (2005--2007) near the equatorial ionospheric anomaly crest region in India. *Annales Geophysicae*, 27(3), 1047 – 1057. <https://doi.org/10.5194/angeo-27-1047-2009>, 2009.
- Balan, N., Otsuka, Y., Nishioka, M., Liu, J. Y., & Bailey, G. J. (2013). Physical mechanisms of the ionospheric storms at equatorial and higher latitudes during the recovery phase of geomagnetic storms. *J. Geophys. Res. Space Physics*, 118(5), 2660–2669, doi:10.1002/jgra.50275.
- Basavaiah, N. (2012). *Geomagnetism: solid earth and upper atmosphere perspectives*. Springer Science & Business Media.
- Basu, S., Basu, S., Huba, J., Krall, J., McDonald, S. E., Makela, J. J., & Groves, K. (2009). Day-to-day variability of the equatorial ionization anomaly and scintillations at dusk observed by GUVI and modeling by SAMI3. *J. Geophys. Res.*, 114, A04302, doi:10.1029/2008JA013899.
- Briggs, B. H. (1984). The variability of ionospheric dynamo currents. *J. Atmospheric and Terrestrial Physics*, 46(5), 419–429, [https://doi.org/10.1016/0021-9169\(84\)90086-2](https://doi.org/10.1016/0021-9169(84)90086-2).
- Bolaji, O., Owolabi, O., Falayi, E., Jimoh, E., Kotoye, A., Odeyemi, O., & Onanuga, K. (2017). Observations of equatorial ionization anomaly over Africa and Middle East during a year of deep minimum. *Ann. Geophys.*, 35(1), 123–132. <https://doi.org/10.5194/angeo-35-123-2017>.
- Chandrasekhar, N.P., Arora, K., & Nagarajan, N. (2014). Characterization of seasonal and longitudinal variability of EEJ in the Indian region. *J. Geophys. Res. Space Phys.*, 119(12), 242–259, <https://doi.org/10.1002/2014JA020183>.
- Chapman, S. (1951). The equatorial electrojet

- as detected from the abnormal electric current distribution above huancayo, peru, and elsewhere, *Archiv Fuer Meteorologie, Geophysik und Bioklimatologie, Serie A*, 4, 368–390, <https://doi.org/10.1007/BF02246814>.
- Chen, C. H., Liu, J. Y., Yumoto, K., Lin, C. H., & Fang, T. W. (2008). Equatorial ionization anomaly of the total electron content and equatorial electrojet of ground-based geomagnetic field strength. *J. Atmospheric and Solar-Terrestrial Physics*, 70(17), 2172–2183, <https://doi.org/10.1016/j.jastp.2008.09.021>.
- Deshpande, M. R., Rastogi, R. G., Vats, H. O., Klobuchar, J. A., Sethia, G., Jain, A. R., Subbarao, B. S., Patwari, V. M., Janve, A. V., Rai, R. K., Singh, M., Gurm, H. S., & Murthy, H. S. (1977). Effect of electrojet on the total electron content of the ionosphere over the Indian subcontinent, *Nature*, 265(5612), 599–600, <https://doi.org/10.1038/267599a0>.
- Dias, M. A. L., Fagundes, P. R., Venkatesh, K., Pillat, V. G., Ribeiro, B. A. G., Seemala, G. K., & Arcanjo, M. O. (2020). Daily and monthly variations of the equatorial ionization anomaly (EIA) over the Brazilian sector during the descending phase of the Solar Cycle 24. *J. Geophysical Research: Space Physics*, 125(9), <https://doi.org/10.1029/2020JA027906>.
- Fambitakoye, O., & Mayaud, P. N. (1976a). Equatorial electrojet and regular daily variation sri. a determination of the equatorial electrojet parameters. *J. Atmospheric and Terrestrial Physics*, 38(1), 1–17, [https://doi.org/10.1016/0021-9169\(76\)90188-4](https://doi.org/10.1016/0021-9169(76)90188-4).
- Fambitakoye, O., & Mayaud, P. N. (1976b). Equatorial electrojet and regular daily variation srii. the centre of the equatorial electrojet. *J. Atmospheric and Terrestrial Physics*, 38(1), 19–26, [https://doi.org/10.1016/0021-9169\(76\)90189-6](https://doi.org/10.1016/0021-9169(76)90189-6).
- Fejer, B.G., Farley, D.T., Woodman, R.F., & Calderon, C. (1979). Dependence of equatorial F region vertical drifts on season and solar cycle. *J. Geophysical Research: Space Physics*, 84, 5792–5796, <https://doi.org/10.1029/JA084iA10p05792>.
- Fejer, B.G. (1997). The electrodynamics of the low-latitude ionosphere: Recent results and future challenges. *J. Atmospheric and Solar-Terrestrial Physics*, 59(13), 1456–1482, [https://doi.org/10.1016/S1364-6826\(96\)00149-6](https://doi.org/10.1016/S1364-6826(96)00149-6).
- Fejer, B.G., & Tracy, B., D. (2013). Lunar tidal effects in the electrodynamics of the low latitude ionosphere. *J. Atmospheric and Solar-Terrestrial Physics*, 103, 76–82, <https://doi.org/10.1016/j.jastp.2013.01.008>.
- Ghosh, P., Otsuka, Y., Mani, S., & Shinagawa, H. (2020). Day-to-day variation of pre-reversal enhancement in the equatorial ionosphere based on GAIA model simulations. *J. Earth, Planets and Space*, 72(1), 1–8, <https://doi.org/10.1186/s40623-020-01228-9>.
- Guizelli, L. M., Denardini, C. M., Moro, J., & Resende, L. C. A. (2013). Climatological study of the daytime occurrence of the 3-meter EEJ plasma irregularities over Jicamarca close to the solar minimum (2007 and 2008). *J. Earth, Planets and Space*, 65, 39–44, <https://doi.org/10.5047/eps.2012.05.008>.
- Gouin, P. (1962). Reversal of the magnetic daily variation at Addis Ababa. *Nature*, 193(4821), 1145–1146. <https://doi.org/10.1038/1931145a0>.
- Hajra, R., Chakraborty, S. K., & Paul, A. (2009). Electrodynamical control of the ambient ionization near the equatorial anomaly crest in the Indian zone during counter electrojet days. *J. Radio Sci.*, 44(3), 1–13. <https://doi.org/10.1029/2008RS003904>
- Huang, Y. N., Cheng, K., & Chen, S. W. (1989). On the equatorial anomaly of the ionospheric total electron content near the northern anomaly crest region. *J. Geophysical Research: Space Physics*, 94(A10), 13515–13525, <https://doi.org/10.1029/JA094iA10p13515>
- Huang, L., Huang, J., Wang, J., Jiang, Y., Deng, B., Zhao, K., & Lin, G. (2013). Guoguo: Analysis of the north--south asymmetry of the equatorial ionization anomaly around 110 E longitude. *J. Atmospheric and Solar-Terrestrial Physics*, 102, 354–361,

- <https://doi.org/10.1016/j.jastp.2013.06.010>.
- Huang, L., Wang, J., Jiang, Y., Huang, J., Chen, Z., & Zhao, K. (2014). A preliminary study of the single crest phenomenon in total electron content (TEC) in the equatorial anomaly region around 120 E longitude between 1999 and 2012. *J. Advances in Space Research*, 54(11), 2200 – 2207, <https://doi.org/10.1016/j.asr.2014.08.021>.
- Iyer, K. N., Deshpande, M. R., & Rastogi, R. G. (1976). The equatorial anomaly in ionospheric Total Electron Content and the Equatorial Electrojet current strength, *Proc. Indian. Acad. Science*, 84A, 129-138, <https://doi.org/10.1007/BF03046803>.
- Jonah, O.F., de Paula, E.R., Muella, M.T.A.H., Dutra, S.L.G., Kherani, E.A., Negreti, P.M.S., & Otsuka, Y. (2015). TEC variation during high and low solar activities over South American sector. *J. Atmos. Sol-Terr. Phys.*, 135, 22-35, <https://doi.org/10.1016/j.jastp.2015.10.005>.
- Khadka, S. M., Valladares, C., Pradipta, R., Pacheco, E., & Condor, P. (2016). On the mutual relationship of the equatorial electrojet, TEC and scintillation in the Peruvian sector. *Radio Sci.*, 51(6), 742–751.
- Khadka, S. M., Valladares, C. E., Sheehan, R., & Gerrard, A. J. (2018). Effects of electric field and neutral wind on the asymmetry of equatorial ionization anomaly. *J. Radio Science*, 53(5), 683–697, <https://doi.org/10.1029/2017RS00642>.
- Liu, J.Y., Chen, Y.I., Chuo, Y.J., & Tsai, H.F. (2001). Variations of ionospheric total electron content during the Chi-Chi earthquake. *J. Geophysical Research Letters*, 28, 1383-1386, <https://doi.org/10.1029/2000GL012511>.
- Ma, G., & Maruyama, T. (2003). Derivation of TEC and estimation of instrumental biases from GEONET in Japan. *Ann. Geophys.*, 21(10), 2083–2093, <https://doi.org/10.5194/angeo-21-2083-2003>.
- Mo, X.H., Zhang, D.H., Liu, J., Hao, Y.Q., Ye, J.F., Qin, J.S., Wei, W. X., & Xiao, Z. (2018). Morphological characteristics of equatorial ionization anomaly crest over Nanning region. *Radio Science*, 53, 37–47, <https://doi.org/10.1002/2017RS006386>.
- Mo, X., & Zhang, D. (2021). A comparative study of the northern and southern equatorial ionization anomaly crests in the East-Asian sector during 2006–2015. *Advances in Space Research*, 68(3), 1461-1472.
- Mungufeni, P., Habarulema, J.B., Migoya-Orué, Y., & Jurua, E. (2018). Statistical analysis of the correlation between the equatorial electrojet and the occurrence of the equatorial ionisation anomaly over the East African sector. *Ann. Geophys.*, 36, 841–853, <https://doi.org/10.5194/angeo-36-841-2018>, 2018.
- Olwendo, O.J., Yamazaki, Y., Cilliers, P.J., Baki, p., & Doherty, P. (2016). A study on the variability of ionospheric total electron content over the East African low-latitude region and storm time ionospheric variations. *Radio Sci.*, 51, 1503–1518, <https://doi.org/10.1002/2015RS005785>.
- Pandey, K., Sekar, R., Anandarao, B.G., Gupta, S.P., & Chakrabarty, D. (2018). On the occurrence of afternoon counter electrojet over Indian longitudes during June solstice in solar minimum. *Journal of Geophysical Research: Space Physics*, 123, 2204–2214, <https://doi.org/10.1002/2017JA024725>.
- Paul, A., Roy, B., Ray, S., Das, A., & DasGupta, A. (2011). Characteristics of intense space weather events as observed from a low latitude station during solar minimum. *J. Geophysical Research: Space Physics*, 116, A10307, <https://doi.org/10.1029/2010JA016330>.
- Rabiu, A.B., Folarin, O.O., Uozumi, T., Hamid, N.S.A., & Yoshikawa, A. (2017). Longitudinal variation of equatorial electrojet and the occurrence of its counter electrojet. *In Annales Geophysicae*, 35, 535–545, <https://doi.org/10.5194/angeo-35-535-2017>.
- Rama Rao, P. V. S., Gopi Krishna, S., Niranjana, K., & Prasad, D. S. V. V. D. (2006). Temporal and spatial variations in TEC using simultaneous measurements from the Indian GPS network of receivers during the low solar activity period of

- 2004–2005. *Annales Geophysicae*, 24, 3279–3292.
- Rastogi, R.G., & Klobuchar, J. A. (1990). Ionospheric electron content within the equatorial F 2 layer anomaly belt. *J. Geophysical Research: Space Physics*, 95, 19045–19052, <https://doi.org/10.1029/JA095iA11p19045>
- Rastogi, R. (2004). Electromagnetic induction by the equatorial electrojet. *J. Geophysical Journal International*, 158, 16–31, <https://doi.org/10.1111/j.1365-246X.2004.02128.x>.
- Romero-Hernandez, E., Denardini, C. M., Takahashi, H., Gonzalez-Esparza, J. A., Nogueira, P. A. B., de Padua, M. B., Lotte, R. G., Negreti, P. M. S., Jonah, O. F., Resende, L. C. A., Rodriguez-Martinez⁶, M., Sergeeva, M. A., Barbosa Neto, P. F., de la Luz³, V., Galera Monico, J. F., & Aguilar-Rodriguez, E. (2018). Daytime ionospheric TEC weather study over Latin America. *Journal of Geophysical Research: Space Physics*, 123(12), doi: <https://doi.org/10.1029/2018JA025943>
- Seemala, G.K., & Valladares C.E. (2011). Statistics of total electron content depletions observed over the Southern American continent for the year 2008. *Radio Sci.*, 46(05), 1-14, <https://doi.org/10.1029/2011RS004722>.
- Siddiqui, T.A., Stolle, C., Lühr, H., & Matzka, J. (2015). On the relationship between weakening of the northern polar vortex and the lunar tidal amplification in the equatorial electrojet. *J. Geophysical Research: Space Physics*, 120, 10006–10019, <https://doi.org/10.1002/2015JA021683>.
- Soares, G., Yamazaki, Y., Matzka, J., Pinheiro, K., Morschhauser, A., Stolle, C., & Alken, P. (2018). Equatorial counter electrojet longitudinal and seasonal variability in the American sector. *J. Geophysical Research: Space Physics*, 123, 9906-9920, <https://doi.org/10.1029/2018JA025968>.
- Stolle, C., Manoj, C., Lühr, H., Maus, S., & Alken, P. (2008). Estimating the daytime Equatorial Ionization Anomaly strength from electric field proxies. *J. Geophysical Research*, 113(A9), <https://doi.org/10.1029/2007JA012781>.
- Talari, P., & Panda, S. K. (2019). Occurrences of counter electrojets and possible ionospheric TEC variations round new Moon and full Moon days across the low latitude Indian region, *Journal of Applied Geodesy*, 13(3), 245-255. <https://doi.org/10.1515/jag-2019-0014>.
- Tsai, H. F., Liu, J. Y., Tsai, W. H., Liu, C. H., Tseng, C. L., & Wu, C. C. (2001). Seasonal variations of the ionospheric total electron content in Asian equatorial anomaly regions. *J. Geophysical Research: Space Physics*, 106(A12), 30363–30369, <https://doi.org/10.1029/2001JA001107>.
- Venkatesh, K., Fagundes, P.R., Seemala, Gopi, K., de Jesus, R., de Abreu, A. J., & Pillat, V. G. (2014). On the performance of the IRI-2012 and NeQuick2 models during the increasing phase of the unusual 24th solar cycle in the Brazilian equatorial and low-latitude sectors. *J. Geophysical Research: Space Physics*, 119, 5087–5105, <https://doi.org/10.1002/2014JA019960>.
- Venkatesh, K., Fagundes, P.R., Prasad, D.S.V.V.D., Denardini, C.M., De Abreu, A.J., De Jesus, R., & Gende, M. (2015). Day-to-day variability of equatorial electrojet and its role on the day-to-day characteristics of the equatorial ionization anomaly over the Indian and Brazilian sectors. *J. Geophys. Res. Space Physics*, 120, 9117–9131, <https://doi.org/10.1002/2015JA021307>.
- Wan, X., Zhong, J., Xiong, C., Wang, H., Liu, Y., Li, Q., Kuai, J., & Cui, J. (2022). Seasonal and Interhemispheric Effects on the Diurnal Evolution of EIA: Assessed by IGS TEC and IRI-2016 over Peruvian and Indian Sectors, *Remote Sens.*, 14(107), <https://doi.org/10.3390/rs14010107>.
- Yizengaw, E., & Moldwin, M.B. (2009). African meridian B-field education and research. *J. Earth, Moon, and Planets*, 104, 237-246, <https://doi.org/10.1007/s11038-008-9287-2>.
- Zhang, R., Liu, L., Yu, Y., Le, H., & Chen, Y. (2020). Westward electric fields in the afternoon equatorial ionosphere during geomagnetically quiet times. *J.*

Geophysical Research: Space Physics,
125,
<https://doi.org/10.1029/2020JA028532>.